Catalytic Oxidation of Allylic Alcohols to Methyl Esters

Gallas-Hulin, Agata; Kotni, Rama Krishna; Nielsen, Martin; Kegnæs, Søren

Published in:
Topics in Catalysis

Link to article, DOI:
10.1007/s11244-017-0821-1

Publication date:
2017

Document Version
Peer reviewed version

Catalytic oxidation of allylic alcohols to methyl esters

Agata Gallas-Hulin [a], Rama Krishna Kotni [a], Martin Nielsen [a] and Søren Kegnæs [a,*]

[a]Technical University of Denmark, Department of Chemistry, 2800 Kgs. Lyngby

* skk@kemi.dtu.dk, +45 45 25 24 02

Abstract:

Aerobic oxidation of allylic alcohols to methyl esters using gold nanoparticles supported on different metal oxide carriers has been performed successfully under mild conditions (room temperature, 0.1 MPa O_2) without significant loss of catalytic activity. The effects of different reaction parameters are studied to find the suitable reaction conditions. All catalysts are characterised by XRD, XRF and TEM. Among these catalysts, Au/TiO_2 showed the most efficient catalytic activity towards the selective oxidation of allylic alcohols to the corresponding esters. Moreover, the same Au/TiO_2 catalyst is used to optimize all the reaction parameters including the significance of the base to promote the reaction. Due to the mild reaction conditions and high conversions as well as selectivity, the utilization of titania-supported gold nanoparticle catalysts represents a benign reaction protocol to synthesize methyl esters from allylic alcohols.

1. Introduction

Over the past decade there has been a strong interest in the alcohol oxidation using gold catalysts [1]. Conventional alcohol oxidation requires toxic metal oxidants and is usually performed at harsh conditions. Although a number of methods have been developed, the search for new facile, cost effective and environmentally benign procedures that can avoid the use of large excess of toxic and

expensive stoichiometric metal oxidants has attracted significant interest [2, 3]. Development of environmentally-friendly catalytic reaction is a crucial part, in particular with respect to the production of fine chemicals. The selective oxidative esterification of alcohol is a key reaction used to produce numerous important chemical intermediates and commodity chemicals [4]. Oxidation with molecular oxygen represents a green and sustainable oxidation method and, therefore, has attracted increasing attention over recent years [5, 6]. Furthermore, over the past decade, gold has been identified as an active catalyst in a variety of reactions, in particular in the selective oxidations of alcohols to its corresponding carbonyl compounds such as aldehydes, carboxylic acids and esters [7-10].

Recent literature shows a growing amount of fundamental research performed with selective alcohol oxidation [11-19]. In particular oxidative esterification of alcohol to methyl esters is one of the good examples of aerobic oxidation reactions leading to the formation of methyl esters which are important in organic chemistry as they are reasonably stable and can be transformed to several other functional groups [20-25]. Among others, allyl alcohol has a particular importance as a potential starting material for the production of acrylic acid or its methyl ester which are widely used for the production of superabsorbent polymers [26]. Christensen et al. oxidized acrolein – aldehyde of allyl alcohol, in methanol under oxygen atmosphere using commercial gold supported on zinc oxide, producing methyl acrylate with 87% selectivity at 97% conversion [27]. Rossi et al. oxidized allyl alcohol in water at room temperature using commercial Au/TiO_2 giving 3-hydroxypropionic acid and acrylic acid with yields 8% and 23.5%, respectively [28]. Yamakawa et al. used various metal oxides and zeolites in hydrogenation of allyl alcohol in methanol with the main product being 3-methoxy-1-propanol at yields of approximately 80% [29].

FIGURE 1

Here we present a new method for the synthesis of methyl esters directly via the selective oxidation of allylic alcohols using molecular oxygen as a terminal oxidant at room temperature. Aerobic oxidation of allyl alcohol (AA) in methanol yielding methyl esters i.e. methyl acrylate (MA) and methyl 3-methoxypropionate (MMP) tested with gold nanoparticles stabilized on different metal oxides as support materials (Al_2O_3, CeO_2, ZrO_2, and TiO_2), see Figure 1. Among all the examined catalysts, commercial Au/TiO_2 catalyst reached the best performance, affording a quantitative combined yield of MA and MMP after 24 h. Therefore, further reaction conditions, such as base loading, choice of base, substrate concentration, heterogeneity of the reaction, and reusability of the catalyst, are studied with Au/TiO_2 as catalyst. The morphological studies of the catalysts were performed by XRD, XRF, TEM and nitrogen physisorption. Quantitative analysis of conversion of allyl alcohol is achieved by GC.

2. Experimental

2. 1. Materials

All the chemicals used for the study are purchased from commercial sources and are used without further purification: allyl alcohol (99%, Aldrich), benzyl alcohol (99%, Aldrich), cinnamyl alcohol (98%, Aldrich), 2-methyl-2-propen-1-ol (99%, Aldrich), trans-2-penten-1-ol (95%, Aldrich), methanol (99.5%, Aldrich), mesitylene (98%, Aldrich), potassium methoxide (25% in methanol, Aldrich), sodium hydroxide (98%, Aldrich), sodium methoxide (30% in methanol, Fluka), methyl acrylate (99%, Aldrich), methyl methoxy propionate (99%, Aldrich) chloroauic acid (III) (99.9%, Aldrich), titanium oxide (99.7%, Aldrich), cerium oxide (99.5%, Alfa Aesar), aluminum oxide (Riedel-De Haenag Seeize-Hannover), zirconium oxide (96%, Aldrich), Au/TiO_2 provided by Mintek, referred as a commercial catalyst. The commercial and the synthesized Au/TiO_2 catalysts had similar catalytic properties, and the following results shown are from the commercial catalyst.

2.2 Preparation of 1 wt% gold catalysts on different supports: 0.02 g of $HAuCl_4 \cdot 3\ H_2O$ is dissolved in 5 mL of water under stirring until homogeneous yellow solution is obtained. Next, saturated solution of sodium bicarbonate is added dropwise until the mixture reached pH 9. After, 0.99 g of support is added and the mixture is left for 1 h under stirring at 50 °C. During this time the solution gradually shifted color from yellow to colorless. After one hour the suspension is filtered and the catalyst is washed with distilled water until no Cl^- ions are detected by addition of $AgNO_3$ solution to the filtrate. Finally the recovered material is dried in air for 24 h and then reduced in 10% H_2 in N_2 at 350 °C for 2 h with a heating ramp of 5 °C/min.

2.3. Catalyst characterization: The analysis of catalyst morphology is examined using transmission electron microscopy (TEM) performed on Tecnai T20 G2 operating at 200 kV. The size of the nanoparticles was calculated from measurements of around 100 particles. Images were taken from several different parts of the samples and at different magnifications.

Crystal analysis is performed by XRD on Huber G670 with $CuK_{\alpha 1}$ radiation for 10 min. The nature of gold species and loading of gold on the support material are determined by XRF analysis on PANalytical Epsilon3-XL.

Nitrogen gas physisorption analysis was performed at 77 K on a Micromeritics ASAP 2020. The surface area was calculated by the Brunauer-Emmett-Teller (BET) method and the pore size distribution were calculated by the Barrett-Joyner-Halenda (BJH) based on the isotherm desorption branch. The total pore volume were determined from the isotherm adsorption branch by a single point read at around P/P0=0.99.

2.4. Catalytic oxidation of allyl alcohol: All reactions are performed on a Radleys carousel in ambient conditions under stirring and oxygen flow. In a typical experiment, a 20 mL glass vessel is loaded with 50 mg of fractionated catalyst (180-355 μm), 2 mmol of allyl alcohol (130 μL), 148 mmol of methanol

(6.0 mL), 0.2 mmol of mesitylene (28 µL) used as internal standard, and 60 µL of potassium methoxide. Samples from the reaction are taken at intervals 0 h, 2 h, 5 h, 24 h, and analyzed using GC (Agilent 7890A).

3. Results and Discussion

3.1. Catalysts characterisation

The XRD analysis of gold on titania catalyst used in the study revealed no characteristic reflexes of gold, what can be seen on Figure 2a. This indicates a uniform distribution and a small size of gold nanoparticles on the surface of titania. The XRD patterns of Au/ZrO_2, Au/CeO_2, and Au/Al_2O_3 catalysts revealed, similar to Au/TiO2 no reflexes of gold. XRD patterns of the Au/ZrO_2, Au/CeO_2, and Au/Al_2O_3 catalysts can be found in Figure S1 in the Supplementary Information. The XRD analysis of the TiO_2 shows the presence of a mixture of anatase and rutile phases (~80% anatase, ~20% rutile). TEM analysis of Au/TiO_2 catalyst showed gold particles of size 2-3 nm, evenly distributed on the support without any tendency to form large clusters, as shown in Figure 2b. TEM analysis of Au/ZrO_2 and Au/CeO_2 revealed similar sizes of the gold nanoparticles and uniform distributions. The size of gold particles in the Au/Al_2O_3 catalyst is slightly larger (5-10 nm). TEM images of the Au/ZrO_2, Au/CeO_2, and Au/Al_2O_3 catalysts can be found in Figure S2 in the Supplementary Information. An overview of the particle sizes for the different catalysts are shown in Table 1. Additional nitrogen physisorption data are shown in the Supplementary Information, Table S1. The BET Surface areas and pore volumes are as expected for metal oxide supports. XRF analysis of the amount of metallic gold on the support revealed the gold loading equal to 0.98-1wt% for all investigated catalysts. Moreover, no characteristic peaks of chlorine are observed in the spectrum indicating the purely metallic form of gold supported on titania (Figure S4). The nature of the supported gold nanoparticles synthesized by

deposition–precipitation has previously been studied in the literature [30]. Details about the characterization of Au/ZrO_2, Au/CeO_2, and Au/Al_2O_3 catalysts using XRD, TEM, XRF and nitrogen physisorption data can be found in the Supplementary Information.

FIGURE 2

3.2. Catalytic activity

In order to examine the activity of the gold catalysts deposited on different support materials (ZrO_2, CeO_2, TiO_2, Al_2O_3,) the oxidation reaction of allyl alcohol is performed at 25 °C and 0.1 MPa O_2 with 10% of the base CH_3OK. Results from the conducted experiments are shown in Table 1. The best results are obtained with Au/TiO_2 which reached 99% conversion after 24 h with the yield towards MMP of 85%. After 24 h the Au/Al_2O_3 catalyst showed the lowest catalytic activity. This could be due to the larger size of the gold particles in the Au/Al_2O_3 catalyst. The size of the gold particles is comparable for the Au/ZrO_2, Au/CeO_2 and Au/TiO_2 catalysts. Surprisingly, the Au/ZrO_2 and the Au/CeO_2 catalysts showed lower activities than the Au/TiO_2 after 24 h. Especially, since the Au/CeO_2 catalyst is known in the literature to be a very active oxidation catalyst even without base. However, the morphology of CeO_2 support is known to play an important role on the catalytic activity. Corma et al. have previously reported that Au/TiO_2 can be a more active than gold on conventional non-nanocrystalline CeO_2 in the oxidation of 3-octanol [16]. Corma et al. also showed that gold supported on nanocrystalline CeO_2 was more active than gold suported on non-nanocrystalline CeO_2 [16].
Next, the role of gold in oxidation of allyl alcohol is investigated. A control experiment is performed in which TiO_2 is used as a catalyst. After 24 h no conversion of allyl alcohol is detected (Table 1) confirming the crucial role of gold in the oxidation reaction. The conversion of allyl alcohol to MA and

then to MMP is shown in Figure 3. The suggested sequential product formation with MA as an intermediate towards MMP is based on the classic Michael addition, which is favorited under, for example, alkaline activation of the nucleophile. However, too high base concentration might shift the equilibrium towards MA and polymerisation through an E1cb intermediate, as shown in Figure 4. As such, MA and MMP are interconvertible.

TABLE 1.

FIGURE 3

FIGURE 4

To get more insight in to the role of base, a set of reactions with different types of bases is performed with Au/TiO_2. All three examined bases are able to drive the reaction successfully, potassium methoxide showed slight superiority (Table 2). The effect of base amount on the oxidation of allyl alcohol is studied by conducting a series of experiments using different loadings of CH_3OK i.e. 0, 5, 10, 15, 20, 50 and 100% under the same reaction conditions. Base is known to assist the oxidation of alcohols on gold supported on titania [31]. Figure 5a depicts the results obtained with different base loadings. The highest yield of MMP is observed for the reaction with 10% of base. When the reaction is performed with increasing base amount, the yield of MMP is observed to be decreasing (19%) gradually. On the other hand, the yield of MA is increased up to approximately 30%. Moreover, the total combined yield of MMP and MA is observed to decrease from quantitative to approximately 50%.

Large amounts of base could facilitate polymerization of MA leading to compounds with high molecular weights which are not detected by GC-MS, see Figure 4.

TABLE 2

FIGURE 5

The effect of substrate to solvent ratio is studied as well. The reaction is performed using different ratios of allyl alcohol to methanol. Data obtained for these experiments is shown in Figure 5b. The highest yield is obtained for substrate to solvent ratio of 1:74 giving 88% yield of MMP after 24 h. It was shown that increasing excess of methanol in the reaction leads to a gradual decrease in the yield of MMP down to 57% with a slight increase in the yield of MA (29%). The possible explanation of this behavior might be the lowered total concentration of base in the reaction mixture for the systems with increased amount of methanol. The mechanism for the formation of allyl alcohol coupling with methanol on an O-activated Au surface has previously been studied by C. M. Friend et al. [32]. The results showed that the product selectivity could be tuned with the concentration of the unsaturated alcohol and methanol.

The reusability of the catalyst is examined by performing several reaction cycles with the same catalyst. After each catalytic cycle, the catalyst is filtered, washed with methanol, dried in air for 24 h, and used in the new reaction cycle. After the fourth cycle, the catalyst is additionally reduced in 10% formier gas at 350 °C for 2 h. Data from these experiments is shown in Figure 6a. It is visible, that the conversion of allyl alcohol decreased with the number of runs from 99% in the first run to 91% in the fourth run. A similar but more significant pattern is observed for the yield of MMP which decreased

from 87% to 48%. On the contrary, the yield of MA increased from 13% to 38%. The total combined yield of MMP and MA is observed to decrease from quantitative to approximately 86% after the fourth run. In the fifth run, when the regenerated catalyst is used, the activity of the catalyst is recovered giving the yields of the products identical those in the first run. The reason for the drop of activity of the catalyst might be due to the formation of carboxylic acid [31], since no morphological changes in the catalyst or size of gold nanoparticles are observed from TEM analysis, as shown in Figure S3 in Supplementary Information.

In order to study the heterogeneity of the reaction, the catalyst is removed from the reaction mixture after 5 h, while all the other parameters remained unchanged. Filtering off the catalyst resulted in inhibition of the reaction with no increase in yield of any of the products after 24 h, which is shown in Figure 6b. This means that even if case of leaching of gold particles from the support material, the activity of the catalyst for the oxidation of allyl alcohol comes from the interaction of gold particles with titanium oxide, and not gold species alone that could leach out of the support into the solution. Furthermore, no gold was observed in the solution by XRF analysis, see Figure S5 in Supplementary Information.

FIGURE 6

Having established the optimal reactions conditions, a scope of the reaction is examined (Table 3). In addition to allyl alcohol, both alkyl and aryl alkene substituted substrates undergo conversion to the desired products in high yields. As such, conducting the reaction with 2-isobutenol afforded the corresponding ester product in a quantitative combined yield (entry 2), and a combined yield of 86% is

obtained with cinnamyl alcohol (entry 3). In addition, employing simply benzyl alcohol also resulted in a quantitative yield of methyl benzoate (entry 4).

Comparing entry 1 with entries 2 and 3, selectivity changes from predominantly favoring the methoxy product in entry 1 to favoring the unsaturated products in the other product mixtures. This is not surprising considering the alkene stabilization effects of both σ-donation and hyperconjugation of the methyl substituent (entry 2) and of π-system conjugation (entry 3) towards nucleophilic attack of the methoxide anion.

TABLE 3

5. Conclusions

In summary, we reported a feasible and efficient way to oxidize allylic alcohols to its methyl esters using gold nanoparticles supported on different metal oxides as catalysts and with oxygen as oxidant at ambient conditions. The study showed superior activity of Au/TiO_2 over the other synthesized catalysts. The reaction parameters, such as base loading, kind of base, substrate concentration, reusability and homogeneity of the reaction are studied. They revealed the high dependence of selectivity of the reaction on the specific reaction parameters. Due to high conversions and high selectivities achieved in the study, gold supported on titania operating at ambient conditions represents a promising and environmentally-friendly approach for oxidation of allylic alcohols to its methyl esters.

6. Acknowledgments: The authors gratefully acknowledge the support of the Danish Council for Independent Research, Grant No. 12-127580, the support of the Lundbeck Foundation

(Lundbeckfonden), Grant No. R141-2013-13244 and the support from VILLUM FONDEN research grant (13158).

7. References

1. Della Pina C, Falletta E, Rossi M, (2012) Chem. Soc. Rev. 41: 350-369

2. Dijksman A, Marion-Gonzalez A, Payeras A M, Arends I W C E, Sheldon R A (2001) J. Am. Chem. Soc. 123: 6826

3. Liu R, Liang X, Dong C, Hu X (2004) J. Am. Chem. Soc. 126: 4112

4. Oliveira R L, Kiyoharaand Liane P K, Rossi M (2009) Green Chem. 11: 1366

5. Mallat T, Baiker A, (2004) Chem. Rev. 104: 3037

6. Kon Y, Usui Y, Sato K (2007) Chem.Comm. 4399

7. Haruta M, Kobayashi T, Sano H, Yamada N, (1987) Chem. Lett. 16: 405

8. Davies S E, Ide M S, Davis R J (2013) Green Chem 15: 17-45

9. Højholt K T, Laursen A B, Kegnæs S, Christensen C H (2011) Top. Catal. 54: 1026-1033

10. Mielby J, Abildstrøm J O, Wang F, Kasama T, Weidenthaler C, Kegnæs S (2014) Angew Chem. Int. Ed. 53: 12513-12516

11. Ryabenkova Y, Miedziak P. J, Dummer N F, Taylor S H, Dimitratos N, Willock D J, Bethell D, Knight D W, Hutchings G J (2012) Top Catal 55: 1283-1288

12. Abad A, Almela C, Corma A, Garcia H (2006) Tetrahedron 62: 6666-6672

13. Zhang Z, Xin L, Qi J, Wang Z, Li W (2012) Green Chem. 14: 2150-2152

14 Yang H, Cui X., Deng Y, Shi F, (2014) RCS Adv. 4: 59754-59758

15. Hackett S F J, Brydson R M, Gass M H, Harvey I, Newman A D, Wilson K, Lee A F (2007) Angew. Chem. Int. Ed. 46: 8593-8596

16. Abad A, Concepcion P, Corma A, Garcia H (2005) Angew.Chem. Int.Ed 44: 4066

17. Christensen C H, Jørgensen B, Rass-Hansen J, Egeblad K, Madsen R, Klitgaard S K, Hansen S M, Hansen M R, Andersen H C, Riisager A (2006) Angew. Chem. Int. Ed. 45: 4648-4651

18. Zope B N, Hibbitts D D, Neurock M, Davis R J (2010) Science 330: 74-78

19. Kumar R, Gravel E, Hagege A, Li H, Jawale D V, Verma D, Namboothiri I N N, Doris E, (2013) Nanoscale, 5: 6491-6497

20. Zheng Su F, Mei Liu Y, Wang L-C, Cao Y, Yong He H, Nian Fan K (2008) Angew. Chem. 120: 340.

21. Abad A, Almela C, Corma A, Garcia H (2006) Chem.Commun. 3178-3180

22. Miyamura H, Yasukawa T, Kobayashi S (2010) Green Chem. 12: 776-778

23. Kegnæs S, Mielby J, Mentzel U V, Jensen T, Fristrup P, Riisager A (2012) Chem. Commun. 48: 2427-2429

24. Mielby J, Kegnæs S, Fristrup P (2012) ChemCatChem 4: 1037-1047

25. Mielby J, Riisager A, Fristrup P, Kegnæs S (2013) Catal. Today 203: 211– 216

26. https://ilbioeconomista.com/2013/07/08/basf-cargill-and-novozymes-realize-another-step-towards-the-biobased-economy/?goback=%2Egde_105359_member_256107668

27. Marsden C, Taarning E, Hansen D, Johansen L, Klitgaard S K, Egeblad K, Christensen C H (2008) Green Chem. 10: 168

28. Della Pina C, Falletta E, Rossi M (2009) ChemSusChem 2: 57-58

29. Yamakawa T, Takizawa M, Ohnishi T, Koyama H, Shinoda S (2001) Catal. Comm. 2: 191-194

30. Zanella R, Delannoy L, Louis C (2005) Appl. Catal. A 291: 62–72

31. Klitgaard S K, DeLaRiva A T, Helveg S, Werchmeister R M, Christensen C H (2008) Catal. Lett. 126: 213-217

32. Zugic B, Karakalos S, Stowers K J, Biener M M, Biener J, Madix R J, Friend C M (2016) ACS Catal. 6: 1833−1839

Figure 1. Depiction of the oxidation of allyl alcohol (AA) in methanol with oxygen at room temperature to methyl esters: methyl acrylate (MA) and methyl 3-methoxypropionate (MMP), using a supported gold catalyst.

Figure 2. (**a**) XRD pattern of the Au/TiO_2 catalyst; red crosses indicate the positions where the characteristic reflexes of gold occur, which are not observed for the tested catalyst; (**b**) TEM image of Au/TiO_2 catalyst used in the study.

Table 1. Results from oxidation of allyl alcohol using different catalysts with 0.1 MPa of O_2 and room temperature.

Figure 3. Conversion of allyl alcohol (AA) to methyl acrylate (MA) and methyl 3-methoxypropionate (MMP) as a function of time catalyzed by Au/TiO_2, 10% CH_3OK, 0.1 MPa O_2 at room temperature.

Figure 4. Detailed mechanism of sequential product formation from MA to MMP based on the classic Michael addition reaction.

Table 2. Results from oxidation of allyl alcohol using 50 mg of Au/TiO_2 as catalyst with 0.1 MPa of O_2 and room temperature.

Figure 5. (**a**) Yields of MA and MMP obtained in the oxidation of allyl alcohol with different base (CH_3OK) loadings at ambient conditions with 0.1 MPa O_2; (**b**) The yields of MA and MMP after 24 hours of the oxidation of allyl alcohol at different allyl alcohol to methanol ratios using standard reaction conditions.

Figure 6. (**a**) Conversion of allyl alcohol into methyl acrylate and methyl methoxypropionate in four cycles using recycled catalyst; in the fifth cycle, the catalyst is regenerated by reduction in 350 °C with 10% formier gas; (**b**) Change of conversion of allyl alcohol catalyzed by commercial Au/TiO_2 to its corresponding esters at ambient conditions with 0.1 MPa O_2 and 10% CH_3OK as a function of time for the system with catalyst and after removal of catalyst after 5 h.

Table 3. Results from oxidations of different allylic alcohols using Au/TiO_2 at standard conditions with 10% CH_3OK after 24h.

312 **Figure 1.**

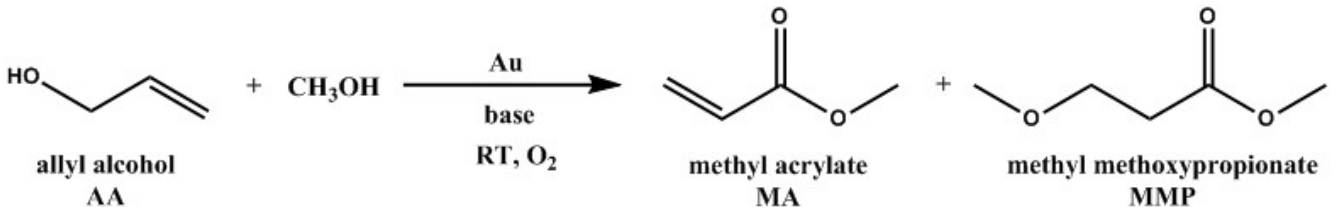

allyl alcohol
AA

methyl acrylate
MA

methyl methoxypropionate
MMP

313

314

315 **FIGURE 2**

316

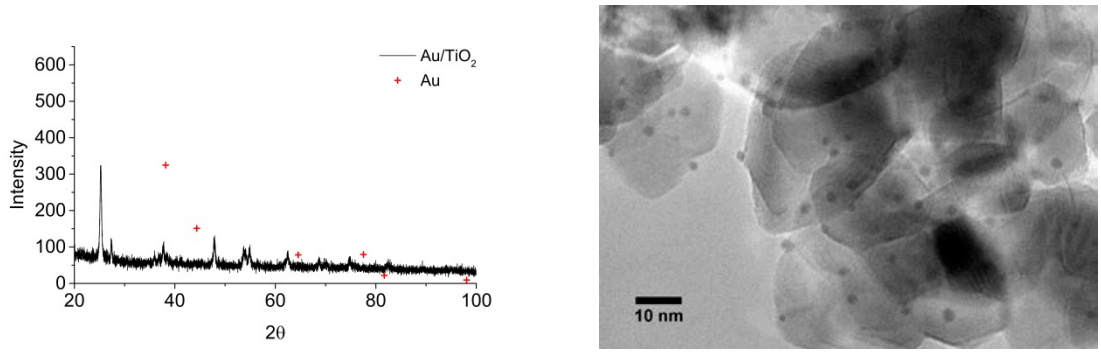

a) **b)**

317

318

Table 1

Catalyst[1]	Particle size (nm)[2]	Conversion (%)[3]		
		2 h	5 h	24 h
Au/ZrO_2	2-3	3	11	35
Au/CeO_2	2-3	10	9	35
Au/Al_2O_3	5-10	5	11	22
Au/TiO_2	2-3	18	33	99
TiO_2	-	0	0	0

[1] 50 mg of catalyst and 10% of base (with respect to allyl alcohol) is used; [2]obtained from TEM analysis; [3]obtained from GC analysis.

Figure 3:

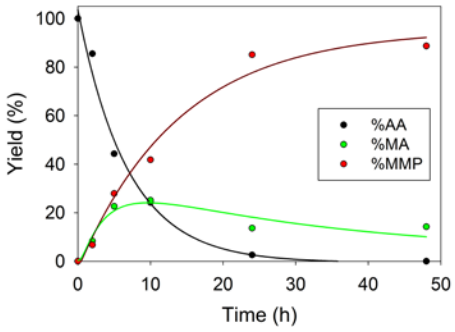

Figure 4

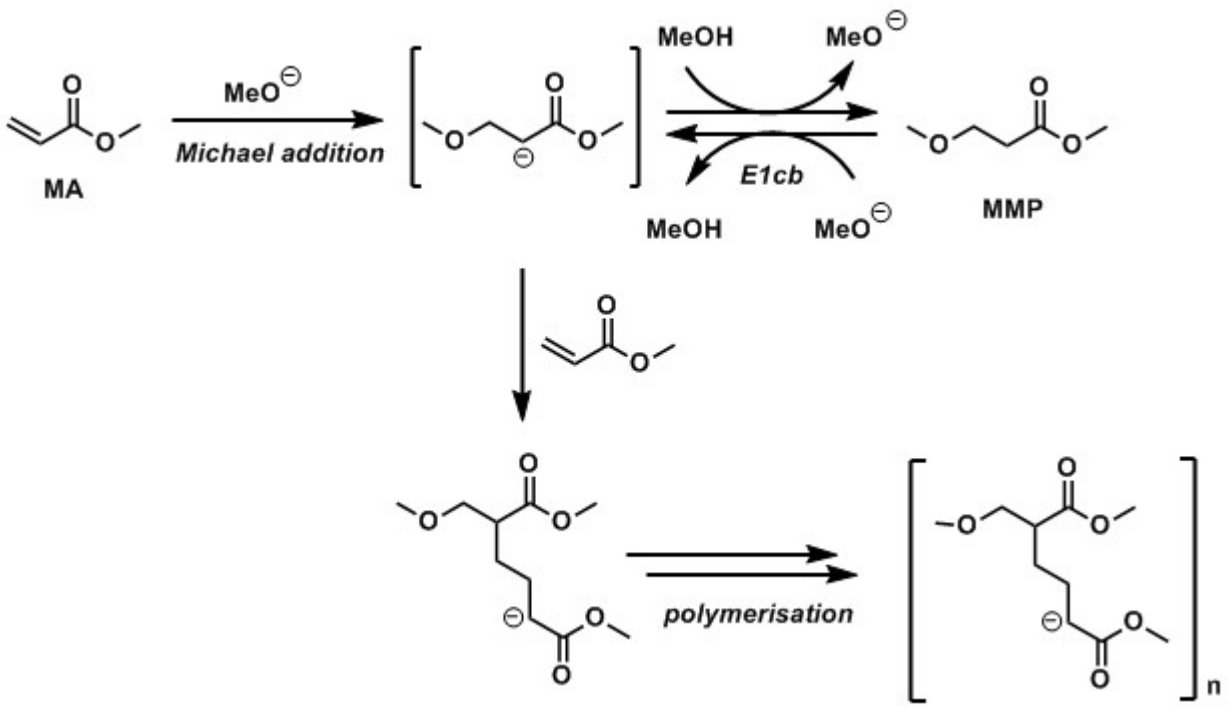
MA
MeO⊖
Michael addition
MeOH
MeO⊖
E1cb
MeOH
MeO⊖
MMP
polymerisation
n

330 **Table 2**

Base[1]	Yield[3] of MMP at 2 h (%)[2]	Yield[3] of MMP at 5 h (%)[2]	Yield[3] of MMP at 24 h (%)[2]
CH_3OK	7	28	85
CH_3ONa	7	17	72
CH_3CH_2ONa	7	17	82

331 [1]10% of base (with respect to allyl alcohol; [2]results obtained from GC analysis.

332

333 **Figure 5**

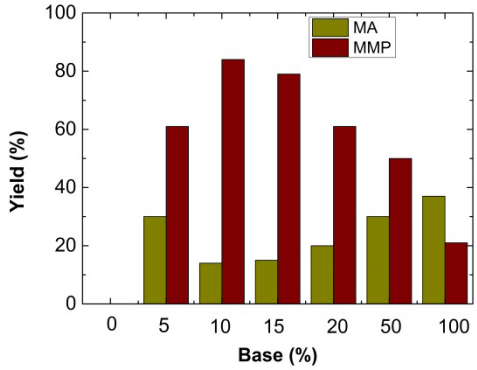

a)

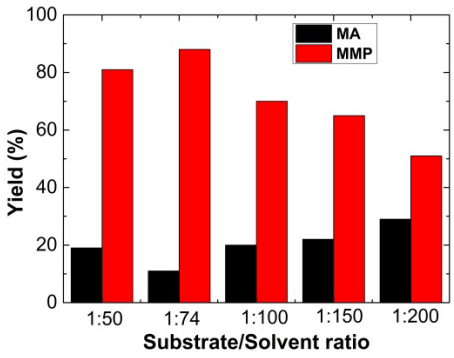

b)

334

335

336 **Figure 6**

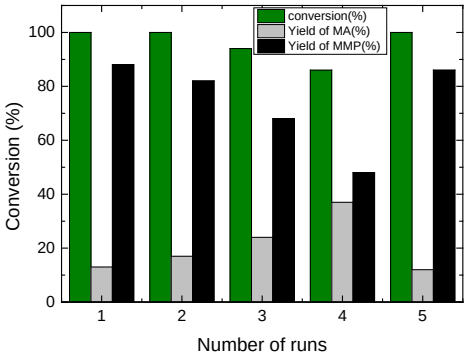

(**a**)

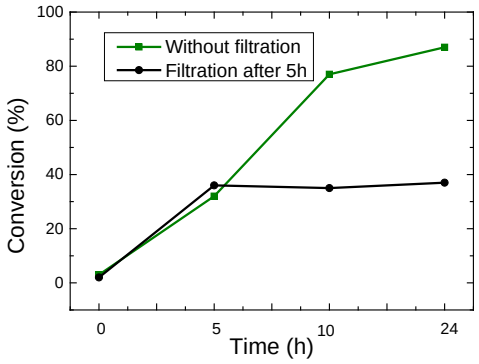

(**b**)

337

338

339 **Table 3**

Substrate	Product A	Product B	Conversion (%)	Yield A-B (%)
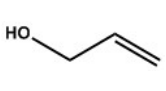	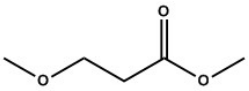	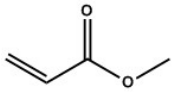	**99**	**85 - 15**
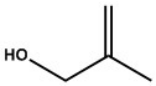	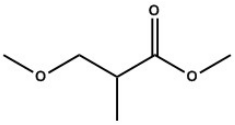	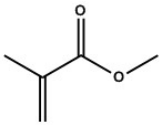	**100**	**24 - 76**
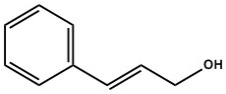	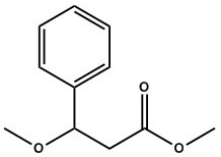	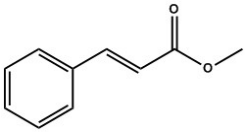	**100**	**7 - 79**
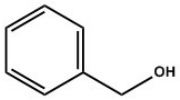	**none**	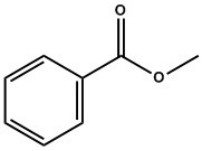	**100**	**n/a - >99**

340